Optical Materials: X 24 (2024) 100369

Contents lists available at ScienceDirect

Optical Materials: X

journal homepage: www.journals.elsevier.com/optical-materials-x

Impact of dicarboxystilbene impurities on the properties of swift heavy ion latent tracks in PET films

Adil Z. Tuleushev [a], Fiona E. Harrison [a], Artem L. Kozlovskiy [a,b], Maxim V. Zdorovets [a,b,*]

[a] Engineering Profile Laboratory, L.N. Gumilyov Eurasian National University, Astana, 010008, Kazakhstan
[b] Laboratory of Solid State Physics, The Institute of Nuclear Physics, Almaty, 050032, Kazakhstan

ARTICLE INFO

Keywords:
PET film
Swift heavy ions
Latent track
Dicarboxystilbene impurity
Photoisomerization
Molecular motor

ABSTRACT

We present a new hypothesis and supporting experimental evidence about the essential role played by small impurities of dicarboxystilbene in the process of UV treatment of PET films irradiated with swift heavy ions (SHI). This treatment both forms highly selective membranes with permeability values comparable to natural ones (the track-UV technique) and sharply accelerates the etching of latent tracks in membrane production (the track-etching technique). We hypothesize (1) that these high permeability value is due to the presence of a molecular motor of an Archimedes screw type in the central part of the latent track formed by photoinduced *trans-cis* isomerization of dicarboxystilbene molecules that are anchored in helical conformations in the latent track; and (2) that the acceleration of etching rates is due to the preferential accumulation of phenanthrene-type molecules in the central part of the latent track due to the existence of a cyclization channel for photoexcited molecules of *cis*-dicarboxystilbene. In the presence of alkali solution, phenanthrene molecules release electrons which behave as strong anions in aqueous solution, catalyzing alkaline hydrolysis of PET molecules in the central part of the track. We present experimental observations of photoinduced changes in transmission light intensity after track-UV light treatment of both pristine and SHI irradiated PET films that confirm the presence of *trans-cis* isomerization of dicarboxystilbene molecules and show their contribution to the formation of new helical conformations in SHI irradiated PET films during the light treatment.

1. Introduction

There is considerable commercial interest in polymer membranes with high ionic selectivity and high transport rates. In Refs. [1,2] such membranes were produced by swift heavy ion (SHI) irradiation of thin polymer films of polyethylene terephthalate (PET) in a vacuum, using Au and Bi ions of energy 2.2 GeV and 1.4 GeV respectively, with subsequent UV light treatment (the 'track-UV' technique). Fluences of $(5 \div 50) \times 10^9$ cm^{-2} were used with mean energy losses of about (16 ± 1.5) keV nm^{-1}. These results have attracted the attention of many researchers [3–10].

For 2 μm thick PET Lumirror® film prepared using the track-UV treatment, ultrafast ion sieving was observed with the film used as a separation membrane in a conductivity cell with an aqueous solution of salts of alkaline and alkaline earth metals and a constant voltage of up to 10 V applied across the film [1,2]. Ultrafast sieving did not occur without the UV treatment and the authors note that ageing of the PET film for at least one week in air after the track-UV treatment contributes to achieving the final result. The transport rate is proportional to the fluence of the SHI irradiation and to the concentration of electrolyte ions and increases rapidly and non-linearly with increasing voltage applied to the membrane. It also increases rapidly and non−linearly with increasing exposure of both sides of the SHI-irradiated film to polychromatic UV/vis light (280 ÷ 600 nm) of flux density of about 4 mW cm^{-2}, for up to 4 h. The authors found that a 12 μm thick PET Hostaphan® film demonstrates higher selectivity, but a transport rate three orders of magnitude lower than that of 2 μm thick film in a similar cell at the same applied voltage. The treatment of the thicker film, however, differed: it was not aged in air, a narrower spectral range of UV light was used (300 ÷ 450) nm, and the maximum exposure was 3 h rather than 4 h.

In [1], the authors suggest that a prerequisite for high selectivity is

This paper was presented at the 12th International Conference on Luminescent Detectors and Transformers of Ionizing Radiation (LUMDETR), June 16-21, 2024, Riga, Latvia.

* Corresponding author. Engineering Profile Laboratory, L.N. Gumilyov Eurasian National University, Astana, 010008, Kazakhstan.
E-mail addresses: mzdorovets@inp.kz, mzdorovets@gmail.com (M.V. Zdorovets).

https://doi.org/10.1016/j.omx.2024.100369
Received 3 September 2024; Received in revised form 23 September 2024; Accepted 27 September 2024
Available online 5 October 2024

the use of SHI with a linear energy loss above 7 keV nm^{-1}. In Ref. [3], a slightly higher threshold of 9 keV nm^{-1} is proposed. The study presented in Ref. [11] of the formation of cylindrical pores in SHI track-etched polyimide film, which is similar in properties to PET film, suggests that Xe and Kr ions of specific energy of about 2 MeV u^{-1} have linear energy losses in a polyimide film of, respectively, 11 keV nm^{-1} and 8 keV nm^{-1}. This raises the possibility that ultrafast sieving membranes might be produced using heavy noble gas ions, which are much more widely used and available than Au or Bi ions.

Consideration of the conditions under which sieving performance was measured for 2 μm and 12 μm films in Refs. [1,2] suggests that it may be possible to improve the performance of thicker films, which are much more widely available than thin ones. The same voltage was applied to both films in the measuring cell, resulting in an electric field in the thin film six times higher than in the thick one. A voltage of 60 V would be required for the electric field in a 12 μm film to be the same as that due to a voltage of 10V applied to a 2 μm film. The measured dependences in Refs. [1,2] of the transmembrane current on the voltage applied to the conductivity cell for films of a given thickness are approximately exponential, so the dependence on the magnitude of the electric field in the film is also exponential. Reducing the electric field by a factor of six therefore has a very strong effect ($\sim e^6 \approx 400$ times) on the value of the ion current through the measurement cell. This accounts for most of the difference found in ion conductivities between the two thicknesses of film, reducing the part that may be due to the difference in thickness from three orders of magnitude to a difference of several times.

The effect of UV illumination has traditionally [12,13] been associated with the photo-oxidation of broken parts of polymer chain molecules destroyed by the SHI in the inner parts of latent tracks [6,9,14–17]. In Refs. [12,13], measurements of the etching breakthrough time in polycarbonate (PC) films irradiated with massive charged fission fragments of ^{252}Cf and then placed in an a.c. conduction cell filled with etching solution showed that, if the irradiated films are aged or exposed to soft UV light before etching, the etching rate increases very noticeably only in the inner core of the latent tracks. The absence of any noticeable effect of UV illumination on the etching rate of the bulk material of the PC film was also noted in Refs. [12,13]. The authors concluded that the combined action of UV and oxygen is important for this increase in etching rate and associated it with photochemical oxidation reactions involving radical groups in the inner core.

In SHI-irradiated PET films, the etching rate of the material along the latent track was found to be up to three orders of magnitude greater than the bulk material [15,18] and the connection with UV illumination confirmed by a number of experiments [19–22]. In contrast to PC films, UV illumination of PET films has some effect on the etching rate of the bulk material, which increases by more than an order of magnitude and also depends on the spectral distribution and light intensity [21].

A number of researchers have sought to investigate the changes in molecular structure leading to such high differences in etching rates via studies of variations in the intensities of absorption lines of various conformations of the ethylene glycol moiety located between neighboring terephthalate groups in the PET polymer chain molecule, in the far infrared region of the spectrum (6–7 μm or about 0.2 eV) [6,9,23,24]. It is well known, however, that the biggest variations between the optical spectra of pristine and irradiated PET films is observed not in the far infra-red but in the visible and near UV (energy range 1.6–4eV): the so-called “red shift” of the absorption edge. There is general agreement that the red shift results from delocalization/the growth of conjugated systems, although there is a divergence of views on how SHI irradiation causes this growth [2,10,24–26].

Using analysis of the optical spectra to investigate the changes in the interaction of light with PET films after SHI irradiation is complicated by the presence of interference fringes [25–27]. One technique for overcoming this difficulty is described in Refs. [28,29] where it is shown that for thin films the spectral transmission function, taking into account the spectral dependences on the coefficient of absorption and refractive index, is given by the geometric mean of continuous envelopes of the positions of the interference maxima and minima. In Ref. [10], we showed that the spectral transmission function obtained by this method is sensitive to changes in the electron distribution in the latent tracks after electrification of the PET film sample.

Since the UV treatment used in Refs. [1,2] is based on an internal photoelectric effect, it leads to a change in the distribution of electrons inside the latent track due to the residual electric field, which exists for a long time after SHI irradiation because of the electret properties of the PET film [7,8,10,30–33]. We would therefore expect to see changes in the spectral transmission function in the visible and near UV parts of the spectrum after UV light treatment.

Furthermore, commercial PET films luminesce [34], and the non-thermal nature of luminescence makes it a sensitive tool for studying electronic processes including those involved in changes in the properties of PET films after SHI irradiation. It is well-known that luminescence increases with growth in the level of delocalization in organic materials [35], making it a promising tool here since the red shift in the absorption edge is due to an increase in delocalization. In Ref. [36] it was shown that an increase in the absorption edge red shift of an irradiated PET film was accompanied by an increase in luminescence intensity.

We note that luminescence has consequences for the correct interpretation of measurements by many commonly-used spectrophotometers (including the one we use), which are designed on the assumption that studied samples are passive light absorbers. Their recording photodiode measures the integral intensity of all the light reaching it, including any luminescence from the film due to the spectrophotometer incident light, but records this as transmitted light of the incident wavelength, regardless of what the actual spectral distribution is. An example of explicit consideration of the luminescent properties of a photoactive material when studying its absorption spectra can be found in the experimental study described in Ref. [37].

The origin of luminescence in PET films remains an open question. Some researchers have suggested that it is the chromophore group of a repeat unit of the PET chain molecule that luminesces [34,38]. Others have suggested that the luminescence is due to trace impurities, basing this hypothesis on experimental results showing that: polycrystalline terephthalic acid (TPA) powders exhibit the same luminescent properties as PET film; the form of luminescence spectra depends on the degree of purity of TPA; and the chromophore TPA groups that coincide with those in PET do not luminesce. These researchers attribute the luminescent properties of both PET films and TPA powders to trace amounts of dicarboxystilbene and dicarboxydiphenyl, by-products of the production of TPA. Together with TPA and ethylene glycol these molecules participate in the polymerization reaction that creates PET, and can be embedded in the PET chain molecule, forming defective luminescent links in them [39,40]. Non-covalent interactions between these molecules and the solid matrix are also possible, due to the band structure of PET film [41].

The impact of impurities on the properties of PET fibers and films is well known. For example, breakage of the polymer chain is associated with the presence of *p*-carboxybenzaldehyde (one of the byproducts of TPA production) in the reaction mixture, and the fact that the actual strength of the polymer material is far lower than the theoretical value is known to be a consequence of the chain heterogeneity of PET molecules [39,40,42–44]. It is also well known that luminescence in an imperfect molecular crystal, which a semi-amorphous PET film is, is associated with defects or impurities [45–49]. These optically active impurities can be either acceptors, receiving and re-emitting the photon energy absorbed by the matrix, or donors, absorbing photons and transferring their energy to the matrix via a non-radiative process. Energy transfers between the matrix and the impurity are influenced by several structural factors, such as the orientation and deformation of the impurity molecule, its environment, the presence or absence of a free molecular volume etc. [50–52].

There are a number of well-known features of stilbene and its derivatives (stilbenes) that distinguish them from other impurities or contaminants in PET film, leading us to hypothesize that stilbenes play a role in the changes that occur inside latent tracks during UV light treatment. We develop our hypothesis as follows.

Stilbenes exhibit classic photoisomerization between *trans* and *cis* isomers, where in the photoexcited state one of the phenyl rings rotates relative to the other around the ethylene bond, transforming planar *trans* and twisted *cis* isomers into one another. Stilbene luminescent properties are mainly due to the *trans* isomer, rather than the *cis* isomer. Due to the difference in the thermodynamic stability of these two isomers, stilbenes usually overwhelmingly occur as *trans* isomers, but after photoisomerization, the *cis* isomers can remain stable. In the presence of oxygen, alongside return to the *trans* isomer, there is a second channel in the photoreaction in which *cis* isomers transform to phenanthrenes. The concentration of phenanthrenes increases with increasing exposure to light. The quantum yield of this reaction is 0.10 or more. Phenanthrenes are known for their easy oxidation and reduction reactions with partial disruption of the aromatic system. Molecules of stilbenes are also characterized by strong bonds with their environment, and can be either donors or acceptors of energy. The photoisomerization reaction of stilbenes demonstrates a strong dependence on the value of the free molecular volume and can be suppressed in favor of other energy transfer channels in the absence of free molecular volume [51,53–55].

It is known that the density of the material in the core of SHI latent tracks in polymer films is significantly lower than in the peripheral regions [1–3,56]. Photoisomerization of stilbene-type impurities present throughout the PET film is therefore most likely to occur in the latent track core, and phenanthrenes will be preferentially produced and accumulate in the central part of the core. The system of π-conjugations in phenanthrenes provide good deep traps for storing excess electrons. These electron traps can be much more easily disrupted by an active agent such as an alkali, than regular fragments of PET chain molecules. Trap disruption is accompanied by the release of free electrons during etching. These electrons behave like anions in an aqueous medium, with a redox potential of −2.87 V enhancing the effect of alkali hydroxyl groups on aryl molecules [57,58]. This would account for the observed high etching rate along the axis of the latent track.

Production of the *cis* isomer by light treatment of PET films is a key part of our hypothesis and would result in a reduction in the level of luminescence in the UV region, and hence a reduction in the level of light detected by the photodiode of our spectrophotometer after light treatment. In this article, we report the results of our experiments to detect photoinduced changes in both pristine and SHI irradiated PET films.

2. Experiment

For investigation we used pristine PET film from industrial rolls of Hostaphan® Mitsubishi Polyester Film RNK12 (Mitsubishi Polyester Film GmbH, Wiesbaden, Germany) with a thickness of 12 μm. SHI irradiation using Kr^{+13} ions of energy 1.33 MeV u^{-1} was performed in normal geometry at the DC-60 heavy ion accelerator in Astana, Republic of Kazakhstan. This energy is sufficient for incident ions to pass through the film [59].

We expect higher fluences to produce stronger effects but want to avoid the complications of overlapping tracks so we chose a fluence comfortably below the onset of overlap. According to the X-ray diffractograms in Ref. [7] the molecular restructuring associated with the overlap of SHI latent tracks in PET films irradiated by Kr ions begins to manifest itself at irradiation exposure of around $(4 \div 5) \times 10^{10}$ cm^{-2}. Accordingly, we used a fluence of 2×10^{10} cm^{-2}, measured using a Faraday cylinder. We also included in our study a sample taken from a roll being prepared for commercial membrane production, which had been irradiated with Kr^{+15} ions of energy 1.75 MeV u^{-1} and a fluence of 4×10^{7} cm^{-2}.

Optical transmission spectra of samples of pristine and irradiated PET films were collected using Jena Specord-250 Plus analytical spectrophotometer (Analytik Jena, Jena, Germany) with a double monochromator across the wavelength range (190 ÷ 1100) nm. To avoid the influence of texture on the spectral dependences of the commercial film samples used in the experiment, they were placed in the spectrophotometer window in such a way that their machine direction coincided with the direction of the slit of the device. Interference fringe-free spectral transmission functions were obtained using the method described in Refs. [28,29], an example of which is shown in Ref. [26]. Unless otherwise stated, spectra were taken in 0.1 nm steps with a scan rate of 1 nm s^{-1}.

We used two forms of light treatment in our studies. First, we used a scheme similar to those in Refs. [6,8,9,60] which treated polymer film samples with the light of two LE-30 lamps (LISMA, Saransk, Russia) with a length of about 90 cm and a power of 30 W each. The manufacturer's description states that the lamps are low-pressure mercury fluorescent lamps with phosphor applied to the inner surface of the bulb that generates UV light in the range from 280 nm to 380 nm (~4.4 eV–3.2 eV) with a spectrum tailing off into the visible (~480 nm/2.6 eV). The distance between the sample and the lamps in Refs. [6,8,9,60] was about 10 cm and a filter of 12 μm pristine PET film was used to protect the film from the part of the UV spectrum above the PET absorption edge. The intensity of the UV illumination was ≈0.5 mW cm^{-2} without the filter and ≈0.4 mW cm^{-2} with it. We used the same lamps, distances and filter to give the same light intensity of about 0.4 mW cm^{-2} which resulted in the temperature of the ambient air near the sample during UV illumination being no more than 30 °C, corresponding well with [6].

We subjected only one side of the sample to light treatment for 30 min, a typical exposure time for the track-etching technique.

The second form of light treatment was developed from our observations in the course of experimental tests to establish optimum conditions for recording spectra. We noticed that repeated measurements on a given sample did not, as might be expected, give identical results. The more the measurement was repeated, the bigger the changes in the spectra. This demonstrates that the spectrophotometer can act not only as a measuring device but also as a low-intensity source of highly monochromatic radiation. In order to use our spectrophotometer as a source of UV light treatment we set it to record the spectra of each sample repeatedly and continuously for 1 h across the range of photon energies from 3.65 eV to 3.97 eV (340 ÷ 312) nm. Before and after this light treatment we recorded the full transmission spectra across the entire range available in our spectrophotometer (190 ÷ 1100) nm.

For technical reasons, direct determination of the light intensity in our experiment is difficult so we estimate it from published data from similar experiments using a monochromator as a light source where experimental set ups permitted such measurements [61–63]. In Ref. [61], a Nernst source of illumination was used as a photon source to study the spectrum of charge traps in electret materials by the photon stimulated discharge current (PSD) method at photon energies up to 1.4 eV (the source power is not specified in the article, however, the usual value in laboratory practice is 50 W). This provided a photon flux on the surface of the studied samples of the order of 10^{15} cm^{-2} s^{-1}, which at the maximum energy of the photons used corresponds to an irradiation intensity of about 0.2 mW cm^{-2}. In Refs. [62,63], a 450 W Xe arc lamp was used as a light source for the PSD study of the effect of UV illumination on the electret properties of polymer films. Light passed through an aqueous IR filter before being decomposed into a spectrum using a monochromator. The resulting photon flux on the sample surface in Ref. [62] at 400 nm (3.1 eV) was measured as 3×10^{14} cm^{-2} s^{-1} nm^{-1}. For a 1 nm s^{-1} scan rate such as used in our experiment, this corresponds to an intensity of 0.15 mW cm^{-2}. In Ref. [63], a similar value of 0.1 mW cm^{-2} nm^{-1} was found. According to the manufacturer's data, the light source in the UV region of the spectrophotometer used by us is a ~40W deuterium lamp, from which we conclude that (0.10 ÷ 0.15) mW cm^{-2} provides an upper estimate of the UVA light intensity in our experiment.

In our second form of light treatment, we have chosen the spectral distribution of the light incident on the sample to be from (3.97 ÷ 3.65) eV. In the first form, the short wavelength boundary of the polychromatic incident light is approximately the same, since the filter very largely cuts off light above 3.97 eV, but at long wave lengths the incident spectrum is that of the LE-30 lamp itself and extends down into the visible. We note that some similar studies used intensities one [1,2] or two [20–22] orders of magnitude higher than in the articles cited above and will consider these, and differences in processing times, when comparing the results of experiments on the effect of light treatment on the properties of PET films.

3. Results

To baseline our studies, the observed UV/VIS/near IR transmission spectra *T(hν)* for pristine and SHI irradiated PET film samples are shown in Fig. 1. Since the spectral changes due to light treatment are small, we follow the approach used in Ref. [64] and present our experimental observations after light treatments in the form of transmission difference spectra. Fig. 2a and b shows the transmission difference spectra *ΔT(hν)* of the pristine and irradiated samples, obtained by subtracting the spectra of samples before light treatment from the spectra after light treatment for each form of light treatment. Negative values of *ΔT(hν)* correspond to a decrease in transmission after light treatment, and positive values correspond to an increase.

It is immediately apparent that the two different light treatments lead to quite different results. Looking first at the results for pristine film after monochromatic light treatment, the difference spectrum in Fig. 2a (black line) exhibits no regular pattern of interference fringes, indicating that the light treatment causes no ablation of the film surfaces (to interferometric accuracy). *ΔT(hν)* is broadly flat and close to zero except for small variations in narrow regions of a few hundredths of eV, spread across the whole spectrum. Fig. 3 (left hand graphs) shows two enlarged fragments of the black line in Fig. 2a with, respectively, positive (Fig. 3a) and negative (Fig. 3b) deviations in *ΔT(hν),* alongside (right hand graphs) the corresponding before/after transmission spectra, showing the patterns of interference fringes generating the difference spectra.

Since the light intensities for both forms of light treatment have broadly similar values, it can be reasonably assumed that ablation is absent in all light treated samples and fringe patterns in the difference spectra show changes in the optical properties of the samples due to the light treatments.

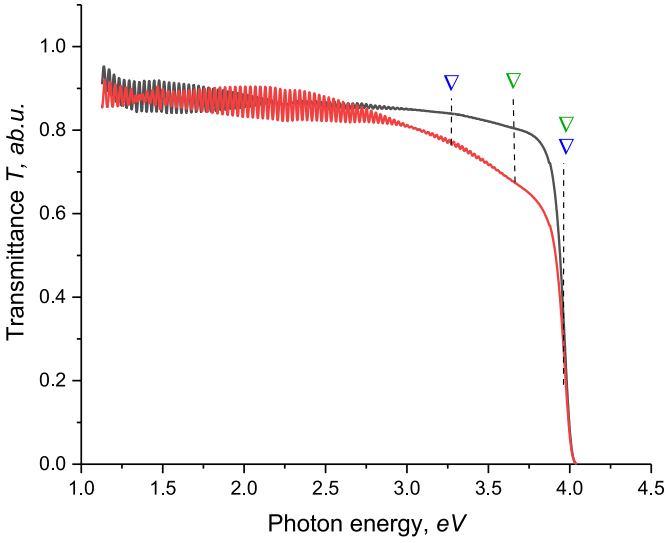

Fig. 1. Experimental transmission spectra *T(hν)* for pristine PET (black line) and after irradiation (red line). Triangles indicate the spectral windows of the two forms of light treatment used: (3.97 ÷ 3.65) eV using the spectrophotometer lamp (green) and (3.97 ÷ 3.25) eV using the LE-30 lamp plus filter (blue). (For interpretation of the references to colour in this figure legend, the reader is referred to the Web version of this article.)

In contrast to the results for pristine film after monochromatic light treatment (Fig. 2a), polychromatic light treatment with the LE-30 lamp (Fig. 2b) results in a regular pattern of interference fringes in *ΔT(hν)* below photon energies of about 3.5 eV, as a result of the fringe pattern in the transmission spectrum shifting in the direction of shorter wavelengths after this light treatment. These fringes also show a positive shift along the intensity axis and exhibit amplitude modulation inherited from the primary transmission spectra and associated with optical activity in the PET films [26]. Another notable difference is the appearance after polychromatic light treatment of a negative minimum in *ΔT(hν) of* amplitude about 1.7 % at about 3.9eV, reflecting a decrease in the intensity of the recorded light.

To investigate this decrease in intensity further, transmission spectra were recorded for two pristine film samples taken from two other rolls (indicated below as 1 and 2), and in addition a sample from roll 1 after irradiation with Kr^{+15} ions of energy of 1.75 MeV u^{-1} and fluence 4×10^7 cm^{-2}. Spectra were measured after polychromatic lamp light treatment as described above. In order to minimize the additional light exposure to the studied samples from the spectrophotometer, spectra were taken in 1 nm steps at a scan rate of 20 nm s^{-1}.

We have previously found it useful to analyze changes in the spectra *T(hν)* of such PET films through the difference function *Δlnα*(hν)* [10], where the non-transmittance coefficient *α*(hν)* characterizes the overall attenuation of the incident light due to both reflection and absorption, and *Δlnα*(hν)* is the logarithm of the ratio of *α*(hν)* values after/before the light treatment. Fig. 4 shows *Δlnα*(hν)* for our three samples. *Δlnα*(hν) = 0* obviously means no change, so corresponds to the value before light treatment. Note that here positive values of *Δlnα*(hν)* correspond to decreases in the intensity of the light recorded by the photodiode of the spectrometer after light treatment.

Although these spectra were taken twenty times faster and with a resolution of only one tenth of those in Figs. 2 and 3, the difference functions of the two pristine PET film samples (Fig. 4, sample 1- red line, and 2 – black line) both show a clear decrease in the intensity of the light recorded by the spectrophotometer in the photon energy range of (3.4 ÷ 4) eV (in both cases the value of the non-transmittance coefficient increases by about 0.08). At lower photon energies (below ~3.5eV) *Δlnα*(hν)* depends only weakly on photon energy and the difference between the two samples can be attributed to the industrial tolerances of technological parameters in film production noted in Ref. [65]. The small oscillations of *Δlnα*(hν)* along the spectra are due partly to real changes in the properties of the films after light treatment but are also an artefact of the 1 nm steps resolution. This coarse resolution makes it impossible to determine interference fringe maxima and minima accurately and consequently introduces errors when cleaning the transmission spectra of interference fringes.

Fig. 4 also shows that irradiation of PET sample 1 with a SHI fluence of 4×10^7 cm^{-2} has no significant effect on the peak in *Δlnα*(hν)* in the region 3.84 eV–3.9 eV, which remains within the envelope of the two pristine film responses. At this fluence, the mean distance between the latent tracks exceeds 1 μm, and the total surface area occupied by them is no more than 0.1 % of the surface of the irradiated film. The similarity of the peaks in *Δlnα*(hν)* for pristine and SHI-irradiated film samples indicates that the decrease in intensity observed after light treatment with LE-30 lamp is connected to a photoactivated process in the molecular structure of the pristine film.

Returning to Fig. 2, the different behaviour of samples exposed to the two different light treatments suggests the presence of interactions between molecules in the PET film and photons in the lower energy tail of the LE-30 lamp spectrum that extends below the PET absorption edge region. Since photons of these energies interact only weakly with repeat units of PET chain molecules, the observed interaction must be with molecules of impurities.

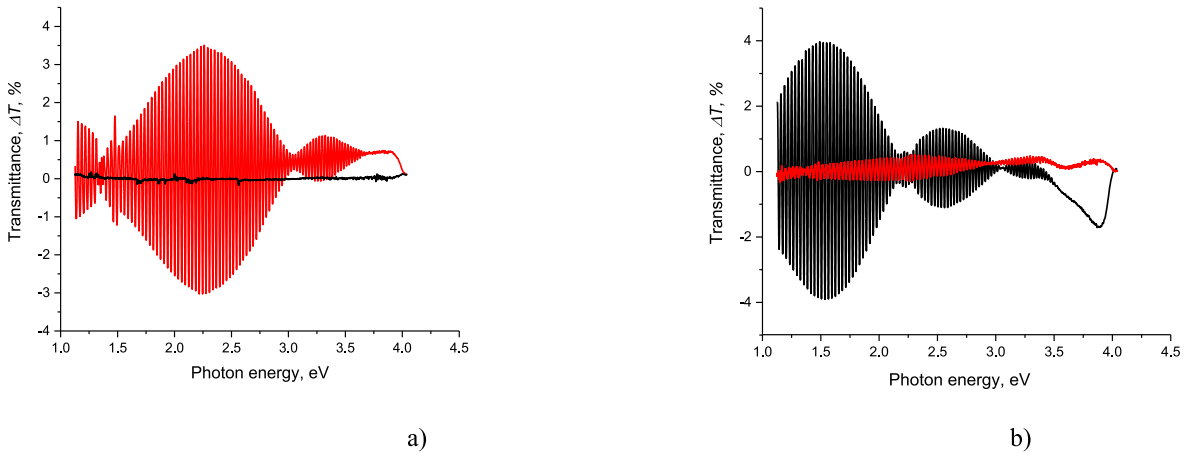

Fig. 2. Difference spectra $\Delta T(h\nu)$ of transmittance of the pristine (black line) and irradiated PET film samples (red line) after illumination with (a) monochromatic light from the spectrophotometer lamp; (b) polychromatic light from the LE-30 lamp. (For interpretation of the references to colour in this figure legend, the reader is referred to the Web version of this article.)

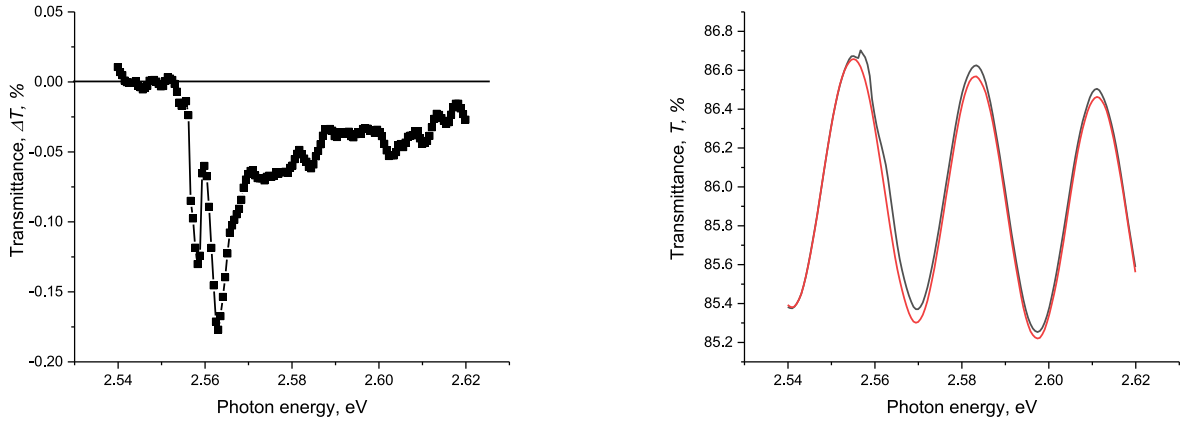

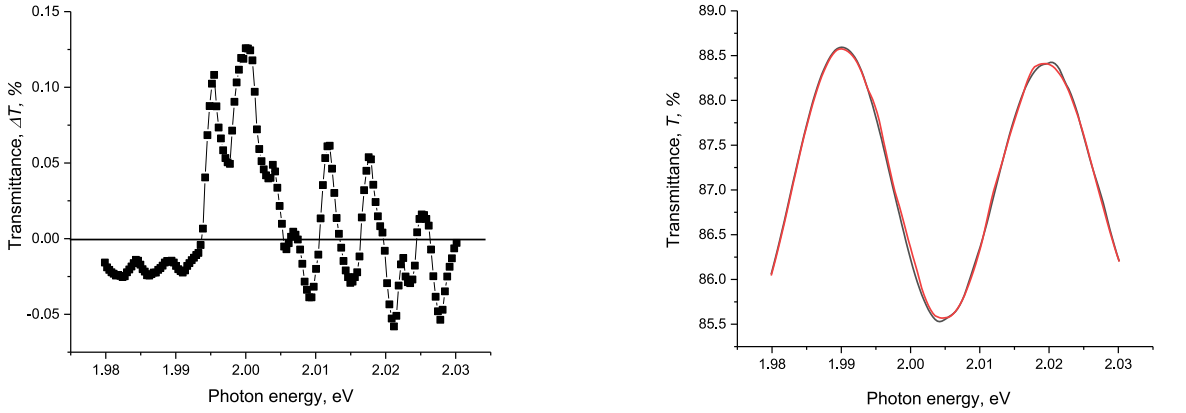

Fig. 3. Examples of a) negative and b) positive deviations of the $\Delta T(h\nu)$ function (left column) as a result of a change in the shape of the interference fringes (right column) of the sample of the pristine PET film before (black line) and after (red line) light of a spectrophotometer lamp treatment. (For interpretation of the references to colour in this figure legend, the reader is referred to the Web version of this article.)

This photoinduced interaction leads to a decrease in intensity of recorded light which, as set out in the introduction, is most plausibly due to the suppression of luminescence present originally, such as would be the case if the polychromatic light treatment resulted in photoisomerization of a molecule from an isomer that luminesces strongly to one that luminesces more weakly. The impurity dicarboxydiphenyl

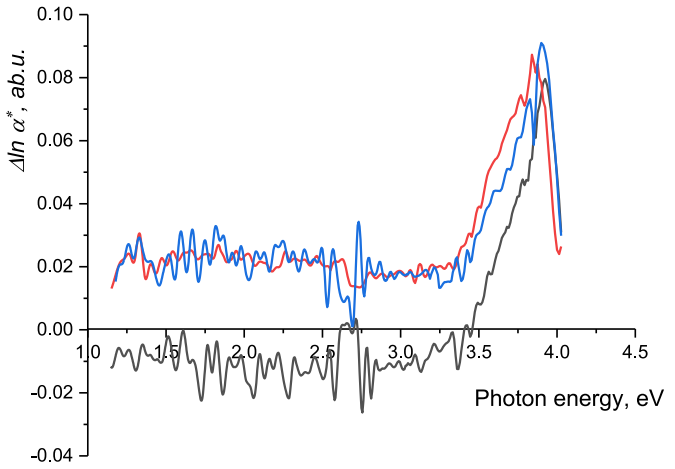

Fig. 4. Difference function *Δlna*(hν)* of two pristine PET film samples (1 - red and 2 - black) before and after polychromatic light illumination with a scan rate of 1 nm. The blue line indicates the similar function for the film sample 1 irradiated with Kr^{+15} ions of 1.75 MeV u^{-1} energy to a fluence of 4×10^7 cm^{-2}. (For interpretation of the references to colour in this figure legend, the reader is referred to the Web version of this article.)

noted in Refs. [39,40] luminesces [66], but due to the symmetry of the molecule does not exhibit photoisomerization. As hypothesized in the introduction, we therefore believe our experimental results are due to *trans–cis* photoisomerization of stilbene-like impurities in the PET film. The isomeric state of stilbene-like molecules is strongly influenced by the surrounding matrix [51]. The planar shape of the repeat units of the PET chain molecule [67] and the texture that develops during the production of commercial films [7] both contribute to the initial configuration of dicarboxystilbene impurities in our samples being predominantly *trans*.

The spectral properties of luminescent impurities in PET films can be assessed using the fluorescence characterization presented in the 3D diagram in Ref. [34], according to which luminescence occurs when a PET film sample absorbs light in the range (300 ÷ 380) nm (4.1 ÷ 3.2) eV. The integral value increases rapidly in the region coinciding with the PET absorption edge, from 300 nm to 320 nm (4.1 ÷ 3.87) eV, then remains broadly constant to 360 nm (3.44 eV) before falling away rapidly. This luminescence excitation window corresponds to the spectral range over which we observe a drop in the intensity in the light recorded by the spectrophotometer after polychromatic light treatment with the lamp LE-30. Both light treatments overlap with this spectral range at higher energies (3.97 ÷ 3.65) eV, much of which falls into the region of strong absorption of the PET polymer matrix [65]. Strong photon absorption by PET molecules leaves few photons available for absorption by molecules of impurities, resulting in a low probability of stilbene photoisomerization. The spectrum of the spectrophotometer as a light source does extend for a short way below the absorption edge, but the lower intensity of this treatment compared to the LE-30 lamp and the integral nature of the recorded spectral intensities result in no detectable sign of photoisomerization for this light treatment.

In contrast, the spectrum of the LE-30 lamp overlaps fully with the lower energy tail (3.65 ÷ 3.25) eV where the intrinsic absorption of PET molecules is small, so a larger number of photons are available to open up a photoisomerization channel. This provides an explanation for the difference in the experimentally observed reactions of identical PET film samples to the two different UV light treatments. In one case, a photoisomerization channel is open but not in the other. Since this channel is only one of the possible competing channels for the transformation of the energy of absorbed photons in stilbenes [51,53–55], the presence of an excitation threshold for the photoisomerization reaction in a PET film does not seem impossible to us.

Fig. 5a shows the difference function *Δlna*(hν)* for pristine PET film

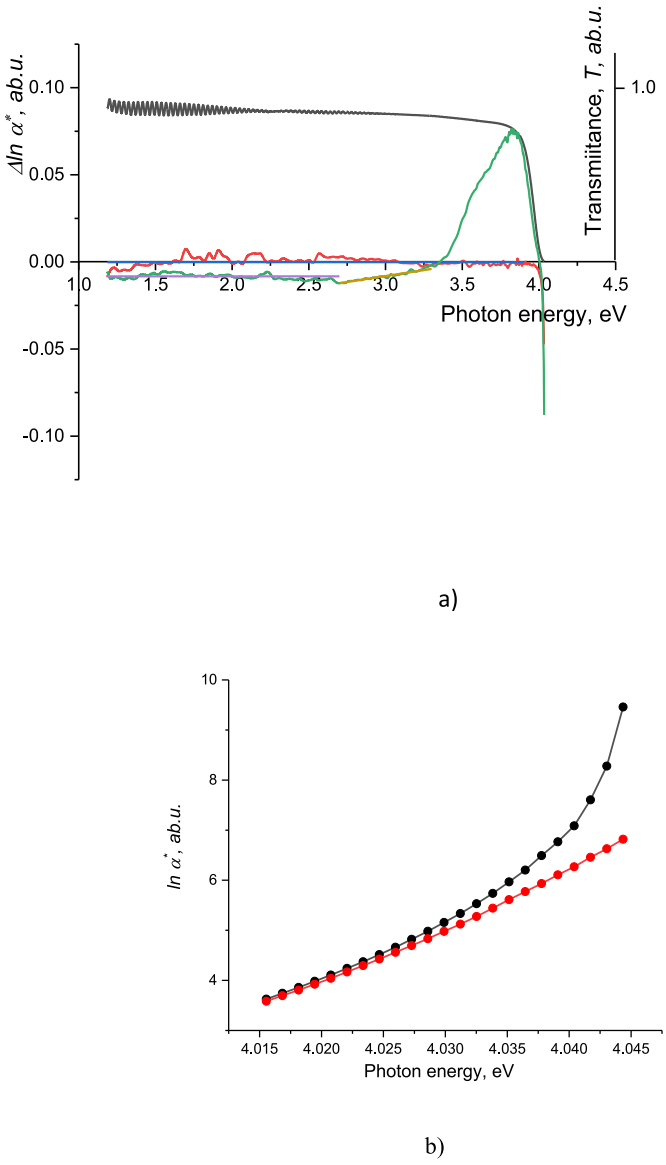

Fig. 5. (a) Difference function *Δlna*(hν) for* pristine PET film samples from roll 2 before and after monochromatic (red) and polychromatic (green) light illumination, taken with a 0.1 nm recording step. The blue line shows the arithmetic mean −0.00015 of the *Δlna*(hν)* function of the sample after monochromatic light illumination at (1.2 ÷ 3.9) eV. The purple line indicates the arithmetic mean −0.0083 of the *Δlna*(hν)* function of the sample after polychromatic light illumination at the interval (1.2 ÷ 2.7) eV. The brown line is an approximation of the difference function of the sample after polychromatic light illumination $\Delta lna^*(h\nu) = 0.015h\nu - 0.0531$ with $R^2 = 0.95$ on the interval (2.7 ÷ 3.3) eV. The black line indicates the transmission spectrum *T (hν)* of the pristine film sample.
b) The behavior of the *lna*(hν)* functions for the pristine film sample before and after light illumination with monochromatic light in the region above 4 eV. The superexponential behavior of this function for the sample before light treatment becomes linear after illumination. The approximation equation is $lna^*(h\nu) = 112.28h\nu - 447.43$ with $R^2 = 0.99$. (For interpretation of the references to colour in this figure legend, the reader is referred to the Web version of this article.)

samples after both forms light treatments, extending to higher photon energies than in Fig. 4 (above 4 eV). For ease of comparison, the transmission spectrum *T(hν)* for the pristine film before light treatment is plotted against the right-hand axis (black line). For both forms of light treatment, *Δlna*(hν)* (green and red lines) drops sharply negative above 4 eV, representing a sharp increase in the current recorded by the

photodiode. We observed very similar behaviour in pristine PET films after electrification [10], which we interpreted using as a ground [68, 69] as a manifestation of the dependence of exciton absorption lines on the value of the local electric field. In Ref. [10], the decrease in the electric field resulted from neutralizing positively charged shallow traps distributed throughout the PET film with electrons injected from negative electrodes. In the experiments here, the decrease is caused by photoexcited electrons moving out of negatively charged deep traps associated with terephthalate moieties. The behavior of $lna^*(h\nu)$ for the pristine film sample before and after treatment with monochromatic light in the region above 4 eV is shown in Fig. 5b (and is the same for polychromatic light).

After monochromatic light treatment, the difference function is almost independent of photon energy over the range (1.2 ÷ 3.9) eV with an average value of −0.00015 (Fig. 5a, blue line). This constant difference function reflects a small overall shift of the transmission spectrum towards higher energies. By analogy with [10], this reflects a small decrease in the random internal electric field after light treatment, due to photoexcited electrons from deep traps being redistributed in the surrounding molecular structures.

After polychromatic light treatment, the lower-energy region of the difference function below 2.7 eV is also almost independent of photon energy with a mean value of −0.0083 (Fig. 5a, purple line). The larger magnitude of the shift indicates a stronger internal photoelectric effect and bigger decrease in the internal electric field for this light treatment. The most likely reason for this is the higher intensity of light in this form of treatment. The difference function is linear with a gradient of 0.015 (Fig. 5a brown line) over the energy range (2.7 ÷ 3.3) eV, showing the presence of an exponential distribution of the probability density of photon absorption, which is typical for the tails of states in amorphous and semi-amorphous materials [70]. This energy range is associated with the PET triplet level zone, hinting at their participation in the reduction of the internal electric field. According to Ref. [38], individual terephthalate moieties have a triplet of levels at 3.0 eV, 3.3 eV, and 3.7 eV, which spread out into a band of states in a solid polymer. In Ref. [37], we observed enhanced light emission appearing in the region from about 2.7 eV to 3.8 eV after SHI irradiation of PET films. We associated this with Dexter annihilation of triplet excitons [45].

Finally, we note that the peak in the difference function $\Delta lna^*(h\nu)$ in the energy region (3.3 ÷ 4) eV corresponds to the maximum of the absorption/excitation spectrum of *trans*-stilbene [71], and the shape of the short-wave side of the peak coincides exactly with the shape of the absorption edge of the PET film, showing that strong photon absorption by PET molecules cuts off the higher energy side of the absorption spectrum of *trans*-stilbene.

Fig. 6 shows the difference function $\Delta lna^*(h\nu)$ for irradiated PET film samples after treatment with monochromatic and polychromatic light, alongside the transmission spectrum $T(h\nu)$ for the irradiated film before light treatment for comparison purposes. We first note that above 4 eV the behaviour of $\Delta lna^*(h\nu)$ is the same for both light treatments, and is the same as the behaviour of pristine PET samples (Fig. 5a), with this behaviour resulting from a decrease in exciton light absorption due to a decrease in the internal electric field in the PET film.

In general, for both of the light treatments, the SHI irradiated PET samples exhibit a stronger photoreaction than the pristine ones, with negative values of $\Delta lna^*(h\nu)$ indicating that the internal electric field is lower after light treatment.

After monochromatic light treatment, the difference function for SHI irradiated PET is almost independent of photon energy at low energies (1.2 ÷ 2.2) eV, where $\Delta lna^*(h\nu) \approx -0.0155$. This reflects a shift in the transmission spectrum towards higher energies due to a decrease in the internal electric field in the sample relative to it before light treatment. Similar behaviour was seen in pristine film, but there the shift was two orders of magnitude smaller (Fig. 5a, blue line). This difference can be explained as follows. In passing through the film, the SHI attracts electrons into the core, leaving the radial periphery zone of the latent track

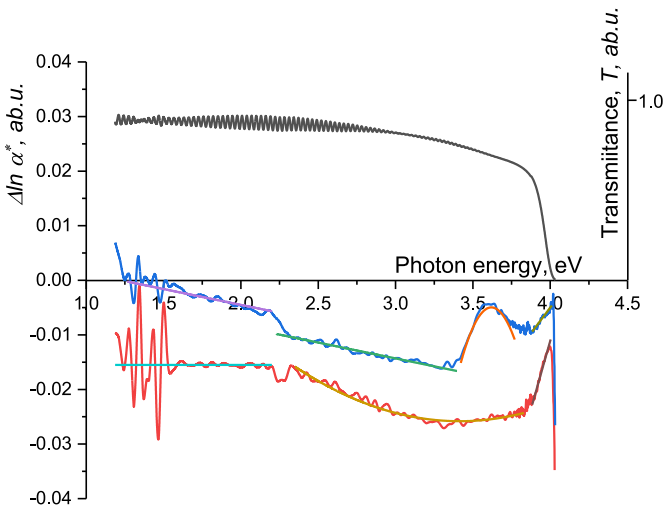

Fig. 6. Difference function $\Delta lna^*(h\nu)$ for PET film samples from roll 2 irradiated with Kr^{+13} ions and fluence xxx, before and after monochromatic (red) and polychromatic (blue) light illumination, taken with 0.1 nm spectral recording step. Approximations of the difference function $\Delta lna^*(h\nu)$ after treatment with monochromatic light are as follows: the light blue line shows the arithmetic mean of −0.0155 over the interval (1.2 ÷ 2.2)eV; the brown line shows the quadratic approximation $\Delta lna^*(h\nu) = 0.0088(h\nu)^2 - 0.0601h\nu + 0.0768$ with $R^2 = 0.96$, a minimum of −0.025 at 3.4 eV and $|\sigma^2| = 56.8$,over the interval (2.35 ÷ 3.83) eV,; the dark brown line shows the linear approximation $\Delta lna^*(h\nu) = 0.1002h\nu - 0.4119$ with $R^2 = 0.98$ over the interval (3.883 ÷ 4.003) eV. Approximations of the difference function $\Delta lna^*(h\nu)$ after treatment with polychromatic light are as follows: the purple line shows the linear approximation $\Delta lna^*(h\nu) = -0.0058h\nu + 0.0071$ with $R^2 = 0.94$ over the interval (1.26 ÷ 2.2) eV; the light green line shows the linear approximation $\Delta lna^*(h\nu) = -0.0058h\nu + 0.0031$ with $R^2 = 0.94$ over the interval (2.23 ÷ 3.4) eV; the orange line shows the quadratic approximation $\Delta lna^*(h\nu) = -0.2599(h\nu)^2 + 1.8814h\nu - 3.4098$ with $R^2 = 0.96$, a maximum of −0.005 at 3.62 eV and $\sigma^2 = 1.92$ over the interval (3.4 ÷ 3.75) eV; the dark green line shows the linear approximation $y = 0.0377x - 0.1558$ with $R^2 = 0.94$ over the interval (3.88 ÷ 4.01) eV. For ease of comparison the transmission function $T(h\nu)$ for the irradiated sample before light treatment is plotted against the right-hand axis (black line). (For interpretation of the references to colour in this figure legend, the reader is referred to the Web version of this article.)

electron-depleted. The further away from the core, the weaker the radial field of the SHI is, and the lower the energy of the electrons that it can remove from traps. In the periphery, electrons are removed only from shallow traps not deep ones, resulting in a more positive bulk environment for the deep traps and thus an increase in their internal local electric fields after SHI irradiation [72]. The subsequent light treatment affects all parts of the sample and the high energy UV photons predominately interact with the deepest traps, freeing electrons from them into the bulk local material. The Franz-Keldysh effect reduces deep trap barriers in the presence of an internal local electric field, which preferentially increases the yield of electrons freed from traps in the peripheral zones, reducing the local electric field in the periphery of the latent tracks.

In the mid-energy part of the spectrum (2.35 ÷ 3.83) eV, the difference function $\Delta lna^*(h\nu)$ after monochromatic light treatment is approximated by a concave quadratic with a minimum near the point (3.4 eV; −0.025). This corresponds to a modulation of $\alpha^*(h\nu)$ by a Gaussian function of the form $\sim \exp(-\nu^2)$. We have previously associated this with density fluctuations arising from a decrease in the level of ordering of terephthalate moieties (from the partial decay of spiral structures formed by SHI irradiation) following a reduction in the internal electric field, leading to deformational fluctuations of the band gap [10]. This Gaussian has a modulus of $\sigma \sim 7.5$ meaning that its dispersion is due to several independent parameters. In our case, this dispersion emerges from the independent contributions of

non-overlapping latent tracks [10].

At high energies (3.883 ÷ 4.003) eV, in the region corresponding to the PET absorption edge, the difference function $\Delta lna^*(h\nu)$ is approximated by a straight line with positive gradient (Fig. 6, dark brown line). This reflects changes in the exponential distribution of tail states in the bandgap below the conduction band after light treatment [68,70]. As noted above, $\Delta lna^*(h\nu) = 0$ means no change in transmission after light treatment, so the observed difference function over this energy range is a counterclockwise rotation of the line $\Delta lna^*(h\nu) = 0$ around a focal point of about 4.1 eV. In Ref. [72] we concluded that this focal point is the value of the bandgap for the electron-enriched core of the latent tracks and that the rotation of $\Delta lna^*(h\nu)$ reflects electrostatic, rather than deformational, changes in the band gap.

After polychromatic light treatment, electrostatic fluctuations in the fields of charged centers are observed in the difference function $\Delta lna^*(h\nu)$ in both the low and high energy regions of the spectrum. At high energies (3.88 ÷ 4.01) eV the linear approximation to $\Delta lna^*(h\nu)$ (Fig. 6, dark green line) is again a counterclockwise rotation of the zero line around a focal point at about 4.1eV, but the angle of rotation is only a third of that for monochromatic light, indicating a smaller reduction in the electric field in the latent track cores. At low (1.26 ÷ 2.2) eV and mid (2.3 ÷ 3.4) eV energies the difference function is well approximated by two parallel straight lines with negative gradient and separated by a vertical shift of 0.04 (Fig. 6, purple and light green lines respectively). The purple upwardly-shifted approximation to $\Delta lna^*(h\nu)$ is a clockwise rotation of the zero line around a focal point at about 1.3 eV, which, drawing on our conclusions in Ref. [10], we associate with the value of the bandgap in the peripheral regions of the latent tracks.

In the narrow energy range (3.4 ÷ 3.75) eV between these linear sections, the difference function is well approximated by a convex quadratic with a maximum near the point (3.62 eV; −0.005) (Fig. 6, orange line). This shows that $\alpha^*(h\nu)$ has been modulated by the Gaussian function $\exp(-v^2)$. We have previously interpreted a concave parabolic dependence of $\Delta lna^*(h\nu)$ as a manifestation of the partial decay of spiral structures formed by SHI irradiation following a reduction in the internal electric field [10]. This suggests that a convex parabolic dependence reflects the formation of additional spiral structures in latent tracks after treatment with polychromatic UV light. This Gaussian has a value of $\sigma \approx 1.4$ which indicates that dispersion is due to a single parameter, and that the polychromatic light treatment has increased the homogeneity of the spiral structures in the latent tracks. This is consistent with the results in Ref. [73] showing that an increase in the length of UV light treatment gives a great improvement in pore size distribution.

The only explanation we can find for these observations is that they are due to *trans-cis* photoisomerization of dicarboxystilbene, the absorption peak of which we observed in $\Delta lna^*(h\nu)$ for pristine film samples after treatment with polychromatic UV light (Figs. 4 and 5). In the process *of trans-cis* isomerization, the molecules of stilbenes have excess energy compared to the rest of the molecular environment (assuming a Boltzmann distribution, their energy corresponds to a temperature of ~600 ÷ 800 K) which leads to heating of the surroundings and enhancing of geometrical changes in the surrounding molecules [37,74]. In the cyclic *trans-cis-trans* process the phenyl rings make a complete revolution around the ethylene bond in four turns. The red shift of about 0.3 eV of the observed peak in $\Delta lna^*(h\nu)$ after polychromatic light treatment for the SHI irradiated sample (at about 3.62eV compared to 3.9 eV in the pristine sample) indicates the growth of non-covalent extended conjugated systems during the formation of additional spiral structures after polychromatic light treatment.

We conclude that the rotation of stilbene molecules during isomerization is responsible for the formation of more homogeneous spiral structures in SHI irradiated PET film samples after polychromatic UV light treatment. Since PET is a condensed medium, these spiral structures should also be subject to rotation. As noted in the introduction, photoisomerization of stilbenes is most likely to occur in latent track cores so this rotational molecular motion will be greatest close to the axes of latent tracks.

Since both left and right rotations are equally probable during isomerization of stilbene molecules, the resulting macroscopic motion of two oppositely rotating Archimedes' screws would be zero. Applying an electric field along the axis of the latent tracks in a SHI irradiated PET film in a liquid introduces an asymmetry which we believe disrupts the balance between left and right rotations. This would lead to a molecular machine unidirectionally moving liquid through the film, providing a new explanation of the high transport rates achieved in Refs. [1,2] for thin SHI irradiated PET films.

4. Discussion

1. Molecular motors based on stilbene-like molecules and powered by light have been actively studied for several decades. Several different types of light-driven motor have been designed and photoisomerization methods used to form supramolecular structures from ensembles of molecules, in which macroscopic effects of unidirectional mechanical motion have been observed. Perhaps the most critical step is the creation, within an ensemble of molecules with the ability to photoisomerize, of conditions where individual molecular motors can operate in a co-operative manner. Homogeneity and a high level of ordering of the molecules, along with the presence of helical structures, are among the most important conditions for synchronizing individual molecular movements. Liquids or gels have been used in most attempts to create light-driven molecular motors, where achieving homogeneity of the molecular ensemble is straightforward, but the creation of ordered structures remains challenging. The steric bulk technique is widely used to create helical molecular configurations via a twisting of the stilbene-like molecule around the double bond. Another technique for creating a helix is anchoring one end of the molecule, allowing the part of the molecule on the other side of the double bond to rotate. Methods of linking molecular motors to macromolecules are being actively studied, with the aim of controlling cooperative movement of large-scale molecular structures through a small number of active molecules that photoisomerize. Since joining molecules using covalent bonds requires chemical synthesis, the use of non-covalent structure-specific interactions is a promising alternative for linking light-driven molecular motors to surrounding macromolecules [75–77] and Refs. therein.
2. We note that the light-treated SHI irradiated PET films studied here possess properties widely recognized as critical for the development of molecular motors. The terephthalate moieties of PET chain molecules in SHI latent tracks are ordered by a radial electric field generated by the passage of the SHI. Coulomb forces attract slow electrons with energies below the ionization potential of PET towards the trajectory of the positively charged ion. Due to the electret properties of PET, this redistribution of electrons from the periphery of the latent track into the core persists for a long time after SHI irradiation. Secondary self-organization into spirals occurs in this ordered ensemble as a result of the dipole-dipole interaction of terephthalate moieties [7,10]. The red shift of the peak in $\Delta lna^*(h\nu)$ for SHI irradiated and polychromatic light treated film compared to its position in pristine polychromatic light treated film indicates that dicarboxystilbene molecules are also involved in the creation of these non-covalent bonds via the two dipole groups on one side of the ethylene double bond. This anchors the dipole groups of dicarboxystilbene within the spiral structures of terephthalate moieties, leaving the second phenyl ring free to rotate. As noted above, rotation is highly dependent on the presence of free molecular volume. It is well-known that the density in the core of the latent tracks is strongly reduced, so free volume sufficient for rotation is much more likely in the core. This suggests that a rotating stilbene molecular motor embedded in a spiral thread-like configuration of PET

molecules could create a torque for the whole spiral, so that it works as an Archimedes screw.

3. The presence of rotational motion of molecular segments in latent tracks in SHI-irradiated PET was confirmed by the X-Ray studies reported in Ref. [7]. These showed that the rotation of mobile terephthalate moieties in the residual electric field of SHI latent tracks forms supramolecular spiral ensembles with non-covalent bonds in the amorphous part of the tracks. The stress along the PET molecular backbone changes and distorts the lattices in crystalline parts through which the chain molecule passes, leading to modulation of the amplitude of the main peak of the crystalline phase in circular X-Ray diffractograms. The presence of modulation for some combinations of SHI charge and irradiation fluence but not for others indicates a variable degree of stability of the spiral conformations: molecular conformations need to be stable for at least the duration of the X-Ray recording time to manifest their presence by modulation of the main peak. Conformations in which the orientations of molecular segments change rapidly compared to the recording time result in X-ray diffractograms of the average intensity of this peak, which is constant at all azimuthal angles of recording. The only available type of motion on these timescales is rotation on σ-hinges. The disappearance at a higher fluence of the modulation of the main peak seen at a lower SHI fluence can be interpreted as confirmation of rotation of spiral conformations inside latent tracks while taking the X-Ray spectra for certain combinations of SHI fluence and ion charge. Since the X-ray diffractograms were taken in light, they provide no insight into whether thermal fluctuations or photoisomerization of stilbene-like molecules causes this rotation. In the experiments in Refs. [1,2], the axial electric field may be driving the rotation of molecular segments by introducing an asymmetry with fixed direction to the previously radially symmetric residual latent track electric field. It could be interesting to take X-ray diffractograms of SHI irradiated film samples, as in Ref. [7], but with an electric field applied across the sample to see whether the field affects the modulation of the peak and could be used to control the rotation of supramolecular ensembles in the latent tracks.
4. Our explanation of the decrease in intensity of the recorded light spectra for both pristine and SHI irradiated PET samples after polychromatic light treatment as due to the suppression of dicarboxystilbene luminescence by photoisomerization can also account for the fact noted in Ref. [21] that UV treatment has a noticeable effect on the etching rate of both latent SHI tracks in PET film and the bulk material. As noted in the introduction, alongside photoisomerization, in the presence of oxygen there is a second channel in the photoreaction of stilbene in which the excited *cis*-isomer transforms to phenanthrene, with a yield that depends on both the spectrum and the intensity of the light treatment. Phenanthrene, which is chemically more active than repeat units of chain PET molecules, will be produced preferentially in the lower-density latent track cores. As PET is an electret, it contains an excess of electrons which accumulate in the extended conjugated systems of phenanthrene [78]. In the presence of an alkaline etchant the middle benzene ring in phenanthrene reacts, freeing electrons which in an aqueous medium act as strong anions and catalyze the decomposition of PET chain molecules, in accordance with results in Ref. [21].
5. Finally, we consider another interesting and unexpected aspect of Fig. 6: the rapid drop in $\Delta lna^*(h\nu)$ over the energy range (2.2 ÷ 2.3) eV for the SHI irradiated sample after polychromatic light treatment (blue line) and the clear depression in $\Delta lna^*(h\nu)$ in the same energy range for the sample after treatment with monochromatic light (red line), indicating a sudden weakening of the internal electric field in this region due to the internal photoelectric effect freeing electrons from deep traps. There is a well-known deep trap in PET at 2.3eV [61,62 and Refs. therein]. In our opinion, the most plausible explanation is that these features are due to the presence of both crystalline and amorphous phases in the PET film, with different refractive indices and, consequently, different dielectric permittivities. Abrupt changes in the value of the internal electric field can only occur at the boundaries between these two phases. The abrupt changes in $\Delta lna^*(h\nu)$ reflect changes in the charge densities at these boundaries after light treatment and are related to the Maxwell-Wagner interphase polarization [33].

5. Conclusion

The peak in the difference function $\Delta lna^*(h\nu)$ for pristine PET after polychromatic UV/vis light treatment at about 3.9 eV confirms the presence of the *trans-cis* photoisomerization reaction of dicarboxystilbene impurities in the PET film. The red shift of the peak by about 0.3 eV and its convex Gaussian shape for SHI irradiated film after the same light treatment reflects the contribution of dicarboxystilbene molecules to the formation of more homogeneous helical structures during the treatment. The strong dependence of geometrical photoisomerization of stilbenes on the presence of free molecular volume results in the preferential formation of new molecular helices in the centers of latent tracks. The ultrafast sieving reported in Refs. [1,2] could be explained by the rotation of stilbene-containing molecular helices. It remains unclear whether such a molecular motor is driven by the applied voltage or by laboratory light, or both. The presence of a cyclization channel in the reaction of photoexcited *cis* dicarboxystilbene leads to the production and accumulation of phenanthrenes around the latent track axis during UV treatment. The acceleration of etching observed in SHI-irradiated PET films after polychromatic UV treatment can be explained as due to the electrons freed by the alkaline destruction of phenanthrene in alkaline solution, which act as strong anions and catalyze the etching reaction along the track axis.

We intend to continue our studies of the rotating molecular structures in the central part of SHI latent tracks in PET films by conducting an experiment similar to that described here, but without using the protective PET film to screen out higher energy UV photons, in line with the experiments described in Refs. [1,2]. This will allow us to investigate the influence of the UVB part of the spectrum of the polychromatic light source on the experiments therein.

Funding

This research received no external funding, and F.E.H. took part in this research as a volunteer.

Institutional review board statement: not applicable

Informed Consent Statement: Not applicable.

Data availability statement

The data presented in this study are available on request from the corresponding author.

CRediT authorship contribution statement

Conceptualization, methodology, formal analysis, investigation, visualization, writing - original draft and review, A.Z.T.; conceptualization, methodology, formal analysis, writing - original draft and review, F.E.H.; investigation, visualization, and review, A.L.K.; methodology, investigation, resources, supervision, project administration, and funding acquisition, M.V.Z. All authors have read and agreed to the published version of the manuscript.

Declaration of competing interest

The authors declare that they have no known competing financial interests or personal relationships that could have appeared to influence

the work reported in this paper.

Data availability

No data was used for the research described in the article.

References

[1] Q. Wen, D. Yan, F. Liu, M. Wang, Y. Ling, P. Wang, P. Kluth, D. Schauries, C. Trautmann, P. Apel, et al., Highly selective ionic transport through subnanometer pores in polymer films, Adv. Funct. Mater. 26 (2016) 5796–5803.
[2] P. Wang, M. Wang, F. Liu, S. Ding, X. Wang, G. Du, J. Liu, P. Apel, P. Kluth, C. Trautmann, Y. Wang, Ultrafast ion sieving using nanoporous polymeric membranes, Nat. Commun. 9 (2018) 569.
[3] F. Liu, M. Wang, X. Wang, P. Wang, W. Shen, S. Ding, Y. Wang, Fabrication and application of nanoporous polymer ion-track membranes, Nanotechnology 30 (2019) 052001.
[4] M. Wang, W. Shen, S. Ding, X. Wang, Z. Wang, Y. Wang, F. Liu, A coupled effect of dehydration and electrostatic interactions on selective ion transport through charged nanochannels, Nanoscale 10 (2018) 18821–18828.
[5] P.Y. Apel, Fabrication of functional micro- and nanoporous materials from polymers modified by swift heavy ions, Radiat. Phys. Chem. 159 (2019) 25–34.
[6] I.V. Blonskaya, O.V. Kristavchuk, A.N. Nechaev, O.L. Orelovich, O.A. Polezhaeva, P.Y. Apel, Observation of latent ion tracks in semicrystalline polymers by scanning electron microscopy, J. Appl. Polym. Sci. 138 (2020) 49869.
[7] A.Z. Tuleushev, M.V. Zdorovets, A.L. Kozlovskiy, F.E. Harrison, Ion charge influence on the molecular structure of polyethylene terephthalate films after irradiation with swift heavy ions, Crystals 10 (2020) 479.
[8] D. Temnov, A. Rossouw, I. Vinogradov, N. Shabanova, T. Mamonova, N. Lizunov, W. Perold, A. Nechaev, Thermo-activation spectroscopy of track-etched membranes based on polyethylene terephthalate films irradiated by swift Xe ions, Radiat. Phys. Chem. 191 (2021) 109868.
[9] I. Blonskaya, N. Kirilkin, O. Kristavchuk, N. Lizunov, S. Mityukhin, O. Orelovich, O. Polezhaeva, P. Apel, Visualization and characterization of ion latent tracks in semicrystalline polymers by FESEM, Nucl. Instrum. Methods Phys. Res. Sect. B Beam Interact. Mater. Atoms 542 (2023) 66–73.
[10] A.Z. Tuleushev, F.E. Harrison, A.L. Kozlovskiy, M.V. Zdorovets, Insight into what is inside swift heavy ion latent tracks in PET film, Polymers 15 (2023) 4050.
[11] C. Trautmann, S. Bouffard, R. Spohr, Etching threshold for ion tracks in polyimide, Nucl. Instrum. Methods Phys. Res. Sect. B Beam Interact. Mater. Atoms 116 (1996) 429–433.
[12] W.T. Crawford, W. DeSorbo, J.S. Humphrey, Enhancement of track etching rates in charged particle-irradiated plastics by a photo-oxidation effect, Nature 220 (1968) 1313–1314.
[13] W.T. Crawford, J.S. Humphrey Jr., W. DeSorbo, Method for making visible radiation damage tracks in track registration materials, Pat. USA № 3612871 (1969).
[14] P.Y. Apel, G. Pretzsch, Investigation of the radial pore-etching rate in a plastic track detector as a function of the local damage density around the ion path, Nucl. Tracks Radiat. Meas. 11 (1986) 45–53.
[15] P. Apel, Track etching technique in membrane technology, Radiat. Meas. 34 (2001) 559–566.
[16] N. Sertova, E. Balanzat, M. Toulemonde, C. Trautmann, Investigation of initial stage of chemical etching of ion tracks in polycarbonate, Nucl. Instruments Methods Phys. Res. Sect. B Beam Interact. Mater. Atoms. 267 (2009) 1039–1044.
[17] K. Froehlich, S. Nasir, M. Ali, P. Ramirez, J. Cervera, S. Mafe, W. Ensinger, Fabrication of soft-etched nanoporous polyimide membranes for ionic conduction and discrimination, J. Memb. Sci. 617 (2021) 118633.
[18] P.Yu Apel, Polymeric materials research with cyclotrons. Proceedings of the 14th International Conference on Cyclotrons and Their Applications (CYCLOTRONS 95), 8-13 Oct. 1995, pp. 136–143. Cape Town, South Africa.
[19] Apel P. Yu, Heavy particle tracks in polymers and polymeric track membranes, Radiat. Meas. 25 (1995) 667–674.
[20] Z. Zhu, Y. Maekawa, H. Koshikawa, Y. Suzuki, N. Yonezawa, M. Yoshida, Role of UV light illumination and DMF soaking in production of PET ion track membranes, Nucl. Instrum. Methods Phys. Res. B. 217 (2004) 449–456.
[21] Z. Zhu, J. Duan, Y. Maekawa, H. Koshikawa, M. Yoshida, Bulk and track etching of PET studied by spectrophotometer, Radiat. Meas. 38 (2004) 255–261.
[22] Z. Zhu, Y. Maekawa, Q. Liu, M. Yoshida, Influence of UV light illumination on latent track structure in PET, Nucl. Instrum. Methods Phys. Res. B. 236 (2005) 61–67.
[23] T. Steckenreiter, E. Balanzat, H. Fuess, C. Trautmann, Chemical modifications of PET induced by swift heavy ions, Nucl. Instruments Methods Phys. Res. Sect. B Beam Interact. with Mater. Atoms 131 (1997) 159–166.
[24] C. Liu, Y. Jin, Z. Zhu, Y. Sun, M. Hou, Z. Wang, Y. Wang, C. Zhang, X. Chen, J. Liu, B. Li, Study of effects in polyethylene terephthalate induced by high energy Ar ion irradiation, Nucl. Instrum. Methods Phys. Res. B 169 (2000) 78–82.
[25] P.Y. Apel, I.V. Blonskaya, O.M. Ivanov, O.V. Kristavchuk, N.E. Lizunov, A. N. Nechaev, O.L. Orelovich, O.A. Polezhaeva, S.N. Dmitriev, Creation of ion-selective membranes from polyethylene terephthalate films irradiated with heavy ions: critical parameters of the process, Membr. Membr. Technol. 2 (2020) 98–108.
[26] A.Z. Tuleushev, F.E. Harrison, A.L. Kozlovskiy, M.V. Zdorovets, Induced gyrotropy in thin PET films before and after swift heavy ion irradiation evidenced from analysis of optical interference fringes, Optical Mater 123 (2022) 111883.
[27] E. Hecht, Optics, 5 ed., Addison-Wesley, 2002.
[28] R. Swanepoel, Determination of the thickness and optical constants of amorphous silicon, J. Phys. E Sci. Instrum. 16 (1983) 1214–1222.
[29] R. Swanepoel, Determination of surface roughness and optical constants of inhomogeneous amorphous silicon films, J. Phys. E Sci. Instrum. 17 (1984) 896–903.
[30] S.A. Saleh, Y. Eyal, Porous tracks along wakes of swift uranium ions in polyimide, Appl. Phys. Lett. 85 (2004) 2529–2531.
[31] S.A. Saleh, Y. Eyal, Morphology of track cores and halos created by swift uranium ions in polycarbonate, Nucl. Instrum. Methods Phys. Res. Sect. B Beam Interact. Mater. Atoms 236 (2005) 81–87.
[32] Y. Takai, T. Osawa, T. Mizutani, M. Ieda, Photoconduction in poly (ethylene terephthalate). I. Mechanisms of carrier generation, J. Polym. Sci. Polym. Phys. 15 (1977) 945–954.
[33] G.M. Sessler, Physical principles of electrets, in: G.M. Sessler (Ed.), Electrets, Springer, Berlin/Heidelberg, Germany, 1980, pp. 13–80.
[34] D.J. Hemker, C.W. Frank, J.W. Thomas, Photophysical studies of amorphous orientation in poly (ethylene terephthalate) films, Polymer 29 (1988) 437–447.
[35] C.B. Murphy, Y. Zhang, T. Troxler, V. Ferry, J.J. Martin, W.E. Jones Jr., Probing Forster and Dexter energy-transfer mechanisms in fluorescent conjugated polymer chemosensors, J. Phys. Chem. B 108 (2004) 1537–1543.
[36] A.Z. Tuleushev, F.E. Harrison, A.L. Kozlovskiy, M.V. Zdorovets, Enhancement of luminescence of PET films after swift heavy ion irradiation, Polymers 15 (2023) 910.
[37] R.J. Sension, S.T. Repinec, A.Z. Szarka, R.M. Hochstrasser, Femtosecond laser studies of the cisstilbene photoisomerization reactions, J. Chem. Phys. 98 (1993) 6291–6315.
[38] J.P. LaFemina, G. Arjavalingam, Photophysics of poly(ethylene terephthalate): ultraviolet absorption and emission, J. Phys. Chem. 95 (1991) 984–988.
[39] R.N. Nurmukhametov, N.V. Ryzhakova, YuYu Yakovlev, Absorption and luminescence spectra of dimethyl terephthalate and poly(ethylene terephthalate), Zhurnal fizicheskoj himii (Russian journal of physical chemistry) 67 (6) (1993) 1142–1145.
[40] R.N. Nurmukhametov, N.V. Ryzhakova, A.Ya Kaminskii, Chain heterogeneity and luminescence of poly(ethylene terephthalate), Vysokomol. Soedin. B 37 (1995) 1096–1099.
[41] V. Coropceanu, X.K. Chen, T. Wang, Z.N. Zheng, J.L. Brédas, Charge-transfer electronic states in organic solar cells, Nat. Rev. Mater. 4 (2019) 689–707.
[42] V.F. Nazimok, L.M. Pivovar, Development of terephthalic acid manufacture, Fibre Chem. 23 (1992) 406–409.
[43] V.V. Korshak, Raznozvennost' polimerov. *Heterogeneity Of Polymers*), Nauka, 1976.
[44] V.V. Korshak, N.M. Kozyreva, G.N. Menchikova, A.V. Gorshkova, E.A. Grigoryan, F.S. D'yachkovskii, The heterogeneity of polymeric units caused by the presence of isotopes, Polym. Sci. 21 (1979) 159–167.
[45] B.P. Zakharchenya, S.A. Permogorov, Excitons in crystals, in: F. Bassani, G.L. Liedl, P. Wyder (Eds.), Encyclopedia of Condensed Matter Physics, Academic Press, 2005.
[46] O.I. Aksimentieva, V.P. Savchyn, V.P. Dyakonov, S. Piechota A, Y.U.Y. U. Horbenko, I.Y.E. Opainych, P.Y.U. Demchenko, A. Popov, H. Szymczak, Modification of polymer-magnetic nanoparticles by luminescent and conducting substances, Mol. Cryst. Liq. Cryst. 590 (1) (2014) 35–42.
[47] V.P. Savchyn, A.I. Popov, O.I. Aksimentyeva, H. Klym, Yu Yu Horbenko, V. Serga, A. Moskina, I. Karbovnyk, Cathodoluminescence characterization of polystyrene-$BaZrO_3$ hybrid composites, Low Temp. Phys. 42 (2016) 597.
[48] I. Karbovnyk, I. Olenych, A. Kukhta, A. Lugovskii, G. Sasnouski, Y. Olenych, A. Luchechko, A.I. Popov, L. Yarytska, Multicolor photon emission from organic thin films on different substrates, Radiat. Meas. (2016), https://doi.org/10.1016/j.radmeas.2015.12.022.
[49] T. Tsebriienko, Anatoli I. Popov, Effect of poly(titanium oxide) on the viscoelastic and thermophysical properties of interpenetrating polymer networks, Crystals 11 (2021) 794.
[50] H.C. Wolf, Energy transfer in organic molecular crystals: a survey of experiments, in: D.R. Bates, I. Estermann (Eds.), Advances in Atomic and Molecular Physics, vol. 3, Academic Press, New York London, 1967, pp. 119–142.
[51] H. Gorner, H.J. Kuhn, Cis-trans photoisomerization of stibenes and stilbene-like molecules, in: D.C. Neckers, D.H. Volman, G. von Bunau (Eds.), Advances in Photochemistry, vol. 19, John Wiley & Sons, 1995.
[52] O. Aksimentyeva, O. Konopelnyk, I. Bolesta, I. Karbovnyk, D. Poliovyi, A.I. Popov, Charge transport in electrically responsive polymer layers, J. Phys.: Conf. Ser. 93 (2007) 012042.
[53] S. Patai, The Chemistry of Alkenes, John Wiley & Sons., 1965.
[54] D.H. Waldeck, Photoisomerization dynamics of stilbenes, Chem. Rev. 91 (1991) 415–436.
[55] G. Stilbenes Likhtenshtein, Applications in Chemistry, Life Sciences and Materials Science, Wiley-VCH Verlag GmbH & Co. KGaA, 2010.
[56] Y. Eyal, K. Gassan, Observation of latent heavy-ion tracks in polyimide by means of transmission electron microscopy, Nucl. Instrum. Methods Phys. Res. B 156 (1999) 183–190.
[57] J.L. Dye, Electrons as anions, Science 301 (5633) (2003) 607–608.
[58] A.K. Pikaev, *Solvatirovannyi Electron V Radiatsionnoi Himii.* (*Solvated Electron in Radiation chemistry.*) M, Nauka, 1969.
[59] J.F. Ziegler, J.P. Biersack, M.D. Ziegler, The Stopping and Range of Ions in Matter, SRIM, Morrisville, NC, USA, 2009.
[60] L.G. Molokanova, YuK. Kochnev, A.N. Nechaev, S.N. Chukova, P.Yu Apel, Effect of ultraviolet radiation on polyethylene naphthalate films irradiated with high-energy heavy ions, High Energy Chem. 51 (3) (2017) 182–188.

[61] J.D. Brodribb, D.M. Huges, T.J. Lewis, The energy spectrum of traps in insulators by photon-induced current spectroscopy, in: Martin M. Perlman (Ed.), Electrets, Charge Storage, and Transport in Dielectrics, The Electrochemical Society, Princeton, 1973, pp. 177–184.
[62] A. Mellinger, F.C. Gonzales, R. Gerhard-Multhaupt, Ultra-violet induced discharge currents and reduction of piezoelectric coefficient in cellular polypropylene films, Appl. Phys. Letters 82 (2003) 254–256.
[63] A. Mellinger, F.C. Gonzales, R. Gerhard-Multhaupt, Photostimulated discharge in electret polymers: an alternative approach for investigating deep traps, IEEE Trans. Dielectr. Electr. Insul. 11 (2) (2004) 218–226.
[64] K.C. Cole, A. Ajji, E. Pellerin, New insights into the development of ordered structure in poly(ethylene terephthalate). 1. Results from external reflection infrared spectroscopy, Macromolecules 35 (3) (2002) 770–784.
[65] A.Z. Tuleushev, F.E. Harrison, A.L. Kozlovskiy, M.V. Zdorovets, Assessment of the irradiation exposure of PET film with swift heavy ions using the interference-free transmission UV-Vis transmission spectra, Polymers 13 (2021) 358.
[66] H. Fukumura, K. Hatanaka, J. Hobley, Laser light interactions with organic solids and their surfaces. Journal of Photochemistry and Photobiology C, Photochemistry Reviews (2001) 153–167.
[67] R. Daubeny, P. de, C.W. Bunn, C.J. Brown, The crystal structure of polyethylene terephthalate, Proc. R. Soc. Lond. A Math. Phys. Sci. 226 (1167) (1954) 531–542.
[68] N.F. Mott, E.A. Davis, Electronic Processes in Noncrystalline Materials, second ed., Oxford University Press, London, UK, 2012.
[69] J.D. Dow, D. Redfield, Electroabsorption in semiconductors: the excitonic absorption edge, Phys. Rev. B 1 (1970) 3358–3371.
[70] J. Tauc, A. Menth, States in the gap, J. Non-Cryst. Solids 8–10 (1972) 569–585.
[71] R.N. Nurmukhametov, Pogloshchenie i liuminestsentsia aromaticheskih soedineniy. Absorption and Luminescence of Aromatic Compounds), Publishing House Chimia, M., 1971.
[72] A.Z. Tuleushev, F.E. Harrison, A.L. Kozlovskiy, M.V. Zdorovets, Urbach rule in the red-shifted absorption edge of PET films irradiated with swift heavy ions, Polymers 14 (2022) 923.
[73] Z. Zhu, Y. Maekawa, Q. Liu, M. Yoshida, Influence of UV light illumination on latent track structure in PET, Nucl. Instrum. Methods Phys. Res. Sect. B Beam Interact. Mater. Atoms 236 (2005) 61–67.
[74] S.T. Repinec, R.J. Sension, A.Z. Szarka, R.M. Hochstrasser, Femtosecond laser studies of the cis-stilbene photoisomerization reactions. The cis-stilbene to dihydrophenanthrene reaction, J. Phys. Chem. 95 (1991) 10380–10385.
[75] N. Koumura, R.W.J. Zijlstra, R.A. Van Delden, N. Harada, B.L. Feringa, Light-driven monodirectional molecular rotor, Nature 401 (1999) 152–155.
[76] T. Van Leeuwen, A.S. Lubbe, P. Štacko, S.J. Wezenberg, B.L. Feringa, Dynamic control of functon by light-driven molecular motors, Nature Rewiews. Chemistry. 1 (96) (2017) 1–6.
[77] D. Roke, S.J. Wezenberg, B.L. Feringa, Molecular rotary motors: unidirectional motion around double bonds, Proc. Natl. Acad. Sci. USA 115 (2018) 9423–9431.
[78] M. Scholz, F. Dietz, M. Mühlstädt, Über die Photocyclisierung der Stilbene und verwandter Verbindungen, Z. Chem. 7 (1967) 329–338.